Journal of the Korean Magnetic Resonance Society **2022**, *26*, 10-16
DOI 10.6564/JKMRS.2022.26.1.010

Investigation on structural symmetry of $CsCoCl_3 \cdot 2H_2O$ crystals by magic-angle spinning ^1H and static ^{133}Cs nuclear magnetic resonance

Sang Hyeon Park,[1] Du Chang Jang,[1] Hara Jeon,[1] Oh Yi Gyeong,[1] Ae Ran Lim[1, 2, *]

[1]Graduate School of Carbon Convergence Engineering, Jeonju University, Jeonju 55069, Republic of Korea
[2]Department of Science Education, Jeonju University, Jeonju 55069, Republic of Korea

Received Mar 14, 2022; Revised Mar 18, 2022; Accepted Mar 19, 2022

Abstract The phase transition temperatures of $CsCoCl_3 \cdot 2H_2O$ crystals are investigated via differential scanning calorimetry (DSC) and thermogravimetric analysis (TGA). Three endothermic peaks at temperatures of 370 K (=T_{C1}), 390 K (=T_{C2}), and 416 K (=T_{C3}) were observed for phase transitions from $CsCoCl_3 \cdot 2H_2O$ to $CsCoCl_3 \cdot 1.5H_2O$, to $CsCoCl_3 \cdot H_2O$, and then to $CsCoCl_3 \cdot 0.5H_2O$, respectively. In addition, the spin-lattice relaxation time $T_{1\rho}$ in the rotating frame and T_1 in the laboratory frame as well as changes in chemical shifts for ^1H and ^{133}Cs near T_{C1} were found to be temperature dependent. Our analyses results indicated that the changes of chemical shifts, $T_{1\rho}$, and T_1 are associated with structural phase transitions near temperature T_{C1}. The changes of chemical shifts, $T_{1\rho}$, and T_1 near T_{C1} were associated with structural phase transitions, owing to the changes in the symmetry of the structure formed of H_2O and Cs^+ ions. Consequently, the structural symmetry in $CsCoCl_3 \cdot 2H_2O$ crystals based on temperature is discussed by the environments of their H and Cs nuclei.

Keywords $CsCoCl_3 \cdot 2H_2O$, spin-lattice relaxation time, thermal property, nuclear magnetic resonance

Introduction

Lower-dimensional magnetic systems have attracted significant attention from researchers.[1-11] In particular, these materials show significant results in the field of physical chemistry; considerable attention is focused on the development of materials suitable for strong energy absorption by solar collectors. However, systems that exhibit one-dimensional Heisenberg-like behavior, such as $CsMnCl_3 \cdot 2H_2O$, have been the primary focus of these researches. When the Mn^{2+} ion in $CsMnCl_3 \cdot 2H_2O$ is replaced with a Co^{2+} ion, anisotropic effects that yield Ising-like behavior are typically observed in the resulting compound.[12-15] The crystal structure of $CsCoCl_3 \cdot 2H_2O$ was first determined by Thorup and Soling;[1] they reported that its crystal structure was identical to that of $CsMnCl_3 \cdot 2H_2O$. In particular, at room temperature, the space group of $CsCoCl_3 \cdot 2H_2O$ was *Pcca* with lattice constants a=0.8914 nm, b=0.7174 nm, c=1.1360 nm, and Z=4. Thus, $CsCoCl_3 \cdot 2H_2O$ can be considered as an example of an Ising-like chain antiferromagnet. The crystal structure of orthorhombic $CsCoCl_3 \cdot 2H_2O$ at room temperature is shown in Fig. 1; as shown in the figure, the Co^{2+} ions in the compound are arranged in the form of –Co–Cl–Co– chains along the a-axis such that each Co^{2+} ion is surrounded by an octahedral coordination

* Address correspondence to: **Ae Ran Lim**, Graduate School of Carbon Convergence Engineering, and Department of Science Education, Jeonju University, Jeonju 55069, Republic of Korea, Tel: 82-63-220-2514; E-mail: arlim@jj.ac.kr

consisting of four Cl^- ions and two O_2^- ions. The chains along the *b*-axis are separated by layers consisting of Cs ions, while those along the *c*-axis were hydrogen-bonded as Cl···H–O–H.[11] Thus, the resulting octahedral structure of $CsCoCl_3 \cdot 2H_2O$ is such that each Cs^+ ion is surrounded by eight Cl^- ions as their nearest neighbors.

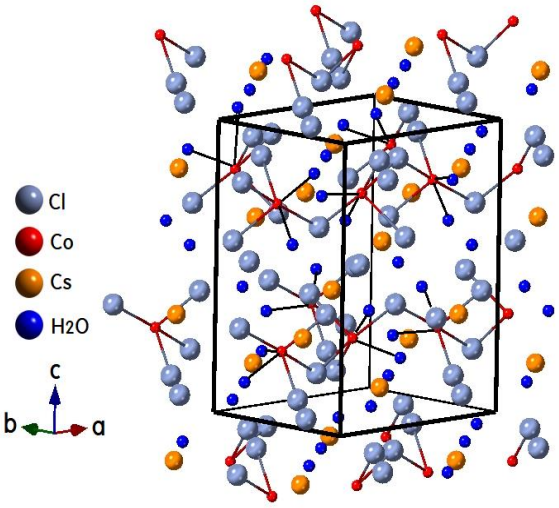

Figure 1. Orthorhombic structure of a $CsCoCl_3 \cdot 2H_2O$ crystal at room temperature (CCDC: 1593038).[1]

Herweijer et al.[3] studied the magnetic properties of $CsCoCl_3 \cdot 2H_2O$ via specific heat, nuclear magnetic resonance (NMR), magnetic susceptibility, magnetization, and antiferromagnetic resonance measurements. In addition, an antiferromagnetic transition at T_N=3.4 K was also previously observed in $CsCoCl_3 \cdot 2H_2O$ using NMR techniques.[2,4] Moreover, the spin-lattice relaxation time T_1 of ^{133}Cs in $CsCoCl_3 \cdot 2H_2O$ was measured near T_N in the laboratory frame by Goto and Kawai.[9] Recently, ^{133}Cs NMR measurements have proved to be valuable in the research on novel materials,[16, 17] and quantum chemical calculations have demonstrated their utility in realizing the structural interpretation of ^{133}Cs NMR spectra.[18, 19]

In this study, the crystal structure of laboratory -grown $CsCoCl_3 \cdot 2H_2O$ was investigated via X-ray diffraction experiments. Moreover, the phase transition temperatures and thermodynamic property of the $CsCoCl_3 \cdot 2H_2O$ crystals were analyzed through differential scanning calorimetry (DSC) and thermogravimetric analysis (TGA). Furthermore, the spin-lattice relaxation times $T_{1\rho}$ in the rotating coordination for ^1H and T_1 in the laboratory coordination for ^{133}Cs in $CsCoCl_3 \cdot 2H_2O$ crystals according to the temperature are discussed. Finally, the structural symmetry of $CsCoCl_3 \cdot 2H_2O$ crystals based on temperature is discussed by the environments of their H and Cs nuclei. The key objective of this study is to clarify the effects of temperature and paramagnetic ions on $CsCoCl_3 \cdot 2H_2O$ crystals with water molecules.

Experimental Procedures

In the experiments, $CsCoCl_3 \cdot 2H_2O$ single crystals were obtained by slow evaporating an aqueous solution containing CsCl and $CoCl_2 \cdot 6H_2O$ in the molar ratio of 1:1. The resulting crystals were light blue in color.

The structure of a single $CsCoCl_3 \cdot 2H_2O$ crystal was confirmed using an X-ray diffractometer (XRD) (Korea Basic Science Institute, Seoul Western Center, Seoul). In addition, the phase transition temperatures were measured using a DSC instrument (TA, DSC 25) by increasing the temperature from 150–600 K; these measurements were conducted at a heating rate of 10°C/min. Furthermore, a TGA device (TA, Q600) was used to perform TGA experiments in order to understand the decomposition phenomena under a N_2 atmosphere at different temperatures with the same heating rate as in the case of the DSC measurements. The changes in the appearance of $CsCoCl_3 \cdot 2H_2O$ single crystals with increasing temperature were captured using an optical polarization microscope wherein the as-grown crystal was placed on a Linkam THM-600 heating stage.

Magic angle spinning (MAS) ^1H NMR spectra and $T_{1\rho}$ values for the $CsCoCl_3 \cdot 2H_2O$ crystal were obtained using a 400-MHz Avance II+ Bruker NMR spectrometer equipped with 4-mm MAS probes (Korea Basic Science Institute, Seoul Western Center). The Larmor frequency $\omega_0/2\pi$ in the MAS ^1H

NMR experiment was set to 400.13 MHz; in addition, the MAS rate was set to 10 kHz to minimize spinning sidebands. The NMR chemical shifts were recorded by using tetramethylsilane (TMS) as the standard. In addition, the static ^{133}Cs NMR spectra and T_1 for the ^{133}Cs nuclei in $CsCoCl_3 \cdot 2H_2O$ single crystal were measured using the same spectrometer; herein, the magnetic field strength was set to 9.4 T with the Larmor frequency $\omega_0/2\pi$ for ^{133}Cs nuclei set to 52.485 MHz. The resonance frequency was recorded using CsCl as the standard. The temperature dependences for ^1H and ^{133}Cs were measured by increasing the temperature from 180–430 K. For the NMR measurements, the temperature of the sample was kept constant with an accuracy of ±0.5ºC while N_2 gas and heater current were passed through the device.

Experimental Results and Discussion

Our X-ray diffraction measurement results showed that the $CsCoCl_3 \cdot 2H_2O$ crystals had an orthorhombic structure with cell parameters a=0.9218 nm, b=0.7288 nm, and c=1.1083 nm; these results are consistent with those previously reported by Thorup and Soling.[1] Three endothermic peaks were observed at 370 K, 390 K, and 416 K in the DSC results as shown in Fig. 2. The mass of the powdered $CsCoCl_3 \cdot 2H_2O$ sample used for DSC measurements was 4.11 mg. In addition, TGA was used to determine whether these three peaks represented structural phase transitions or phase melting temperatures. The TGA curve for $CsCoCl_3 \cdot 2H_2O$ is shown in Fig. 3; herein, the mass of $CsCoCl_3 \cdot 2H_2O$ sample used was 7.08 mg. The loss in mass during the TGA experiment was first noted at approximately 350 K. This aspect was characterized by a loss in the weight of the compound. The loss in the weight of $CsCoCl_3 \cdot 2H_2O$ (Mw=334.23 mg) was observed at high temperatures. The amount of the obtained solid residues was calculated considering the molecular weight of the compound by using Eq. (1)

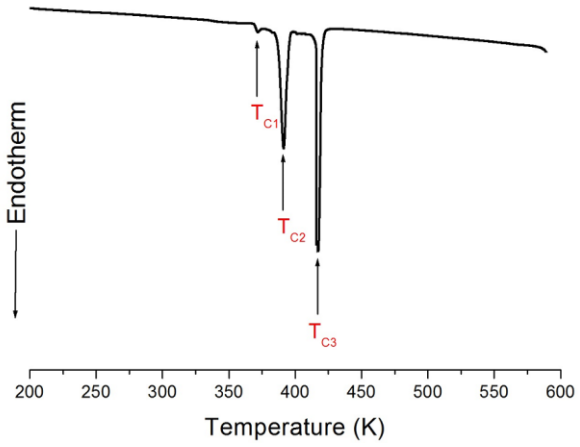

Figure 2. DSC thermogram of $CsCoCl_3 \cdot 2H_2O$ crystals.

$[CsCoCl_3 \cdot 1.5H_2O\ (s) + 0.5H_2O\ (g)] / CsCoCl_3 \cdot 2H_2O = 97.30\ \%$

$[CsCoCl_3 \cdot H_2O\ (s) + H_2O\ (g)] / CsCoCl_3 \cdot 2H_2O = 94.61\ \%$

$[CsCoCl_3 \cdot 0.5H_2O\ (s) + 1.5H_2O\ (g)] / CsCoCl_3 \cdot 2H_2O = 91.91\ \%$

$[CsCoCl_3\ (s) + 2H_2O\ (g)] / CsCoCl_3 \cdot 2H_2O = 89.22\ \%$ (1)

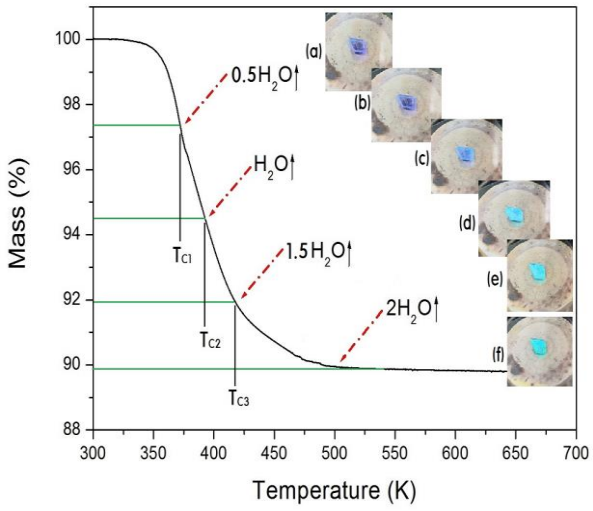

Figure 3. TGA curve of $CsCoCl_3 \cdot 2H_2O$ single crystals. Inset: The color variation of the crystals at temperatures of (a) 293 K, (b) 353 K, (c) 373 K, (d) 403 K, (e) 473 K, and (f) 573 K obtained using an optical polarization microscope.

The thermal decompositions around 370 K and 390 K, which were also indicated via the obtained DSC peaks, were accompanied by partial escape of

$0.5H_2O$ and H_2O, respectively. The residue of the partial products was 97.30 % and 94.61 %, which suggests that $CsCoCl_3{\cdot}2H_2O$ undergoes decomposition during the dehydration process; in particular, it was observed that $CsCoCl_3{\cdot}2H_2O$ loses 1.5 molecules of water of crystallization transforming to $CsCoCl_3{\cdot}0.5H_2O$ at 416 K. Furthermore, the original $CsCoCl_3{\cdot}2H_2O$ sample underwent complete thermal decomposition to $CsCoCl_3$ near 500 K. Based on the obtained DSC and TGA results, the endothermic peaks near 370 K (=T_{C1}), 390 K (=T_{C2}), and 413 K (=T_{C3}) for $CsCoCl_3{\cdot}2H_2O$ decomposition could be attributed to the incremental loss of H_2O molecules from the crystal. Our optical polarization microscopy results for $CsCoCl_3{\cdot}2H_2O$ showed that the crystals are light blue in color at room temperature and that this color changes as the temperature is increased. In particular, the crystals retain their light blue color between 293 and 373 K, and start turning slightly opaque at approximately 403 K, before becoming fully opaque around 573 K. These changes in color with increasing temperature can also be attributed to the loss of H_2O molecules from the crystal.

The temperature dependences of the chemical shifts in the MAS ^{1}H NMR spectrum of $CsCoCl_3{\cdot}2H_2O$ crystals were recorded; these are shown in the inset in Fig. 4. In the temperature range of 180 K-370 K, the ^{1}H chemical shift was nearly constant at 7 ppm, however, above 370 K, the ^{1}H chemical shift increased rapidly to approximately 25 ppm. This phenomenon could be attributed to the effect of the paramagnetic (Co^{2+} ions) near H as a certain amount of H_2O was lost.

The $T_{1\rho}$ values were obtained using a $\pi/2-\tau$ sequence by changing the spin-locking pulses: the $\pi/2$ pulse widths for ^{1}H were 26 μs and 9 μs below and above 370 K, respectively. It was observed that the areas of the MAS ^{1}H NMR spectra for different delay times at each temperature followed a single exponential function. The corresponding decay curve for spin-locked proton magnetization is characterized by $T_{1\rho}$ as follows:[20-22]

$$P(\tau) = P(\infty)\exp(-\tau/T_{1\rho}), \quad (2)$$

where $P(\tau)$ and $P(\infty)$ are the areas under the NMR signal at times $\tau=0$ and $\tau=\infty$, respectively. Using the slopes of the plots for the area under the NMR signal for different delay times, the ^{1}H $T_{1\rho}$ data for $CsCoCl_3{\cdot}2H_2O$ was obtained for each temperature; as shown in Fig. 4, the ^{1}H $T_{1\rho}$ values were in the range of 5–20 μs and were dependent on temperature. It can also be observed that $T_{1\rho}$ decreases abruptly after T_{C1} at which temperature the last remaining $0.5H_2O$ is lost. Similar to the rapid change in the ^{1}H chemical shift above T_{C1}, the reduction in ^{1}H $T_{1\rho}$ is likely a result of the effect of the presence of the paramagnetic Co^{2+} ion in the vicinity as a certain amount of H_2O is lost. The ^{1}H $T_{1\rho}$ values in the case of the paramagnetic ions are smaller than those in the absence of paramagnetic ions because $T_{1\rho}$ is inversely proportional to the square of the magnetic moment of the paramagnetic ions.[19, 23] Thus, the ^{1}H $T_{1\rho}$ values were driven by fluctuations in the magnetic dipole of the paramagnetic Co^{2+} ions.

The static NMR spectra of ^{133}Cs (I=7/2) in a

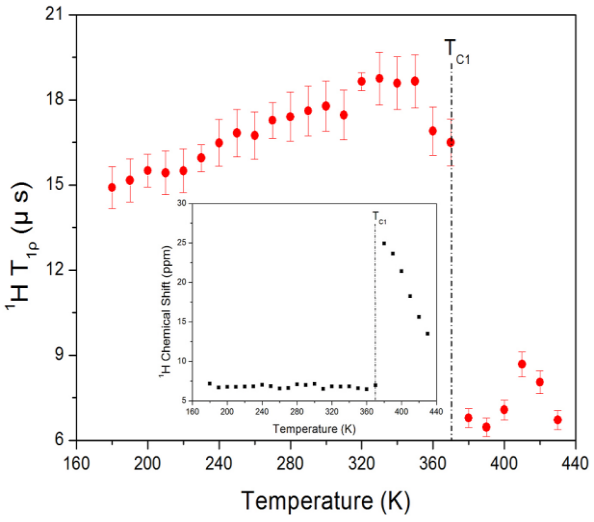

Figure 4. MAS ^{1}H NMR spin-lattice relaxation times $T_{1\rho}$ in $CsCoCl_3{\cdot}2H_2O$ with increasing temperature. Inset: Temperature dependency of ^{1}H chemical shifts as a function of temperature.

$CsCoCl_3{\cdot}2H_2O$ single crystal at various temperatures were measured at a Larmor frequency $\omega_0/2\pi$ =52.485 MHz; these are as shown in Fig. 5. The seven

resonance lines are due to the quadrupole interaction of the ^{133}Cs nucleus; consequently, the NMR spectrum for ^{133}Cs consists of six satellite resonance lines and one central resonance line. The resonance frequencies for ^{133}Cs obtained via NMR were measured in the temperature range of 180–430 K. The Cs NMR spectra were obtained using CsCl as the reference; their resonance frequencies were recorded with increasing temperature in the high frequency direction by the paramagnetic Co^{2+} ions. These shifts in the ^{133}Cs signal are caused by dipole-dipole interactions between the magnetic moments of the paramagnetic Co^{2+} atoms and those of the Cs^+ nuclei. Seven Cs resonance lines were observed in the NMR spectra for temperatures in the range of 180–360 K, while only one Cs resonance line was observed above 370 K. The realization of only one Cs resonance line at temperatures above T_{C1} indicates that the phase transition above this temperature is the dynamic averaging of the crystal electric field and the cubic symmetry field around Cs,

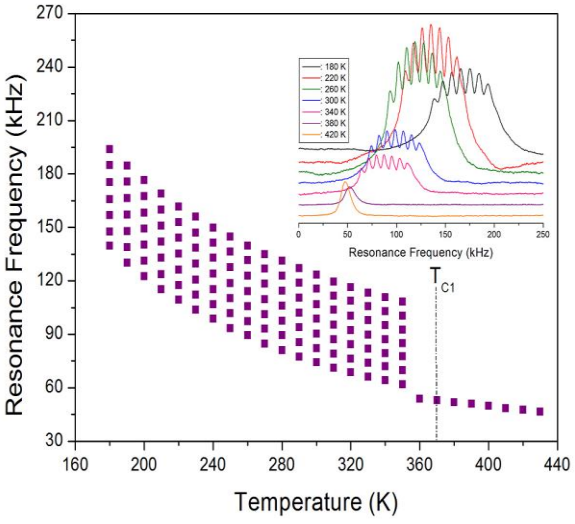

Figure 5. Static ^{133}Cs NMR resonance frequencies for a $CsCoCl_3 \cdot 2H_2O$ crystal with increasing temperature. Inset: ^{133}Cs NMR spectra at several temperatures.

which, in turn, conveys that the surrounding Cl^- sites around Cs^+ in $CsCoCl_3 \cdot 2H_2O$ are symmetrical above T_{C1}. Further, the changes in the structural geometry of the surrounding sites around Cs are caused by the loss of water molecules around the Cs nucleus, and they play an important role at high temperature.

The magnetization recovery trace for ^{133}Cs in the $CsCoCl_3 \cdot 2H_2O$ crystals with quadrupole relaxation is represented as the sum of four exponential functions and can be expressed as follows:[24, 25]

$$[P(\infty) - P(\tau)] / P(\infty) = 0.048 \exp(-0.476\ P_1\tau) + 0.818 \exp(-1.333\ P_1\tau) + 0.050 \exp(-2.381\ P_1\tau) + 0.084 \exp(-3.810\ P_1\tau) \quad (3)$$

where $P(\tau)$ is the nuclear magnetization of the central transition among several transitions and P_1 is the transition probability for $\Delta m = \pm 1$. The return to thermal equilibrium is characterized by the four terms in Eq. (3). However, because the spin system rapidly returned to thermal equilibrium depending on the spin temperature similar to our high-temperature experiments, the relaxation is described using just a single relaxation time T_1. Thus, the saturation recovery data at high temperatures can be satisfactorily fitted using the following relationship with a single exponential function:[26, 27]

$$[P(\infty) - P(\tau)]/P(\infty) = \exp(-P\tau). \quad (4)$$

Thus, the relaxation time T_1 for ^{133}Cs can be obtained in terms of 1/P.

The T_1 values for the ^{133}Cs nuclei in the crystals were measured using the $\pi/2-\tau-\pi/2$ pulse sequence method. The nuclear magnetization $P(\tau)$ of the ^{133}Cs nuclei at time τ after the application of $\pi/2$ pulses was obtained based on the saturation recovery sequence. The width of $\pi/2$ pulses used for ^{133}Cs in our experiment was 4.1–6 μs. The saturation curves of the ^{133}Cs nuclei were measured at various delay times; in addition, the slopes of these curves were obtained as a function of delay time in the range of 1 μs–400 ms as shown in Fig. 6. The relaxation time, T_1, was calculated directly from the slope of the plot for log $[P(\infty) - P(\tau)] / P(\infty)$ versus time τ. The saturation curve for the central line of ^{133}Cs is represented by a combination of four exponential functions. The temperature dependences of the ^{133}Cs transition rates P_1 and P_2 were fitted using Eq. (3), while the ^{133}Cs relaxation times at low temperatures were obtained in terms of P_1 ($T_1 = 1/1.333P_1$).

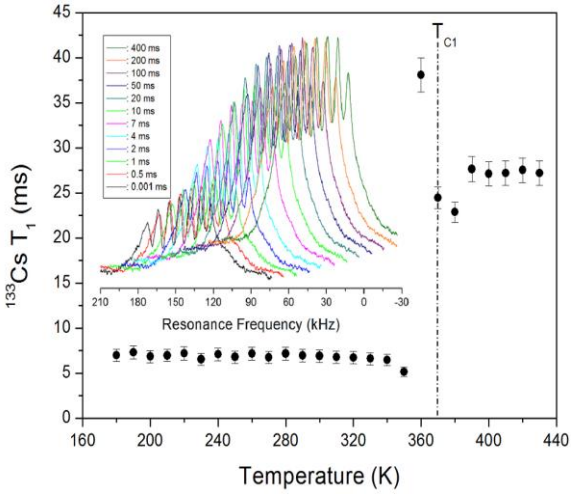

Figure 6. Temperature dependency of the spin-lattice relaxation time T_1 for ^{133}Cs in a $CsCoCl_3 \cdot 2H_2O$ single crystal. Inset: Saturation curves for ^{133}Cs with delay times of 1 μs–400 ms at 300 K.

These temperature dependence plots of the ^{133}Cs T_1 for $CsCoCl_3 \cdot 2H_2O$ crystals is shown in Fig. 6; in particular, the T_1 values of the ^{133}Cs nuclei were nearly constant below 360 K. However, T_1 changes suddenly at the phase transition temperature of 370 K (=T_{C1}), which is consistent with the ^{133}Cs NMR spectra and DSC results. T_1 value increases near 360 K and then decrease again near 370 K. Above that temperature, it remains at a similar value. The increase in T_1 at 360 K is thought to be due to the breaking of the bond before loss of H_2O around Cs. As previously indicated, the change of T_1 near T_{C1} (=370 K) is related to the changes in the geometry of the H_2O and Cl^- surrounding the Cs^+ ions. Moreover, the rapid increase in T_1 above 370 K indicates that H_2O is lost around Cs, which hinders the energy transfer compared to that at lower temperatures.

Conclusions

The structure and lattice constants of $CsCoCl_3 \cdot 2H_2O$ crystals were determined via x-ray diffraction measurements. In addition, the thermal property and phase transition temperature of these crystals were investigated via TGA and DSC. It was observed that phase transitions occur in the crystals at temperatures of 370 K, 390 K, and 416 K. In particular, the endothermic peak at 370 K (=T_{C1}) was related to the phase transition from $CsCoCl_3 \cdot 2H_2O$ to $CsCoCl_3 \cdot 1.5H_2O$. Furthermore, the changes in the temperature dependence of ^{1}H chemical shifts and $T_{1\rho}$ near T_{C1} were associated with structural phase transitions owing to the loss of H_2O molecules, which, in turn, caused the distortion of the octahedral structure of H_2O molecules surrounding Co^{2+}. The resonance lines in the ^{133}Cs spectra reduced from seven to one near T_{C1}, which could be attributed to this structural transformation. Thus, the changes in the temperature dependence of ^{133}Cs T_1 near T_{C1} observed in our study were related to changes in the symmetry of the structure formed of the four Cl^- ions and two H_2O about the Cs^+ ion. At temperatures above T_{C1}, the environments around H and Cs changed owing to H_2O loss; specifically, as a certain amount of H_2O was lost, ^{1}H $T_{1\rho}$ was considerably affected by Co^{2+} around H, and as H_2O was lost around Cs, T_1 increased owing mainly to the influence of the $4Cl^-$ ions around Cs^+. Consequently, the thermodynamic properties and structural geometry of the $CsCoCl_3 \cdot 2H_2O$ single crystals were studied by analyzing these environments.

Acknowledgements

This research was supported by the Basic Science Research program through the National Research Foundation of Korea (NRF) funded by the Ministry of Education, Science, and Technology (2018R1D1A1B07041593, 2016R1A6A1A03012069).

References

1. N. Thorup, H. Soling, *Acta Chem. Scand.* **23**, 2933 (1969)
2. W.J.M. de Jonge, K.V.S. Rama Rao, C.H.W. Swuste, A.C. Botterman, *Physica.* **51,** 620 (1971)
3. Herweijer, W.J.M. de Jonge, A.C. Botterman, A.L.M. Bongaarts, J.A. Cowen, *Phys. Rev.* B. **5,** 4618 (1972)
4. A.L.M. Bongaarts, B. van Laar, *Phys. Rev.* B. **6**, 2669 (1972)
5. J. Flokstra, G.J. Gerritsma, A.J.W.A. Vermeulen, *Phys. Letters* A. **44**, 485 (1973)
6. T. de Neef, *J. Phys. Soc. Japan* **37**, 71 (1974)
7. J.N. McElearney, *Solid State Commun.* **24**, 863 (1977)
8. K. Kopinga, Q.A.G. van Vlimmeren, A.L.M. Bongaarts, W.J.M. de Jonge, *Physica* B. **86-88**, 671 (1977)
9. T. Goto, T. Kawai, *J. Phys. Soc. Japan* **50**, 3531 (1981)
10. Y. Ajiro, K. Adachi, M. Mekata, *J. Mag. Mag. Mater* **31-34**, 1141 (1983)
11. I. Mogi, T. Okamoto, N. Kojima, T. Ban, I. Tsujikawa, *J. Phys. Soc. Japan* **55**, 987 (1986)
12. A.K. Ghosh, *Phys. Rev.* B **80**, 214418 (2009)
13. Y.B. Kudasov, A.S. Korshunov, V.N. Pavlov, D.A. Maslov, *Physics-Uspekhi* **55**, 1169 (2012)
14. A.K. Ghosh, *J. Magn. Magn. Mater.* **324**, 2907 (2012)
15. J. Strecka, O. Rojas, S.M. de Souza, *Phys. Letter* A. **383**, 2415 (2019)
16. D.J. Kubicki, D. Prochowicz, A. Pinon, G. Stevanato, A. Hofstetter, S.M. Zakeeruddin, M. Gratzel, L. Emsley, *J. Mat. Chem.* A **7**, 2326 (2019)
17. F. Ji, Y. Huang, F. Wang, L. Kobera, F. Xie, J. Klarbring, S. Abbrent, J. Brus, C. Yin, S.I. Simak, I.A. Abrikosov, I.A. Buyanova, W.M. Chen, F. Gao, *Advan. Funct. Mater.* **30**, 2005521 (2020)
18. J. Czernek, J. Brus, *Chem. Phys. Letters* **684**, 8 (2017)
19. C.J. Moon, J. Park, H. Im, H. Ryu, M.Y. Choi, T.H. Kim, J. Kim, *Bull. Korean Chem.* Soc. **41**, 702 (2020)
20. A. Abragam, *The Principles of Nuclear Magnetism* (Oxford: Oxford University Press, 1961)
21. A.R. Lim, *Solid State Commun.* **312**, 113862 (2020)
22. H. Kwon, S. Lee, S. Hong, A.N. Kiyonga, J.-J. Yi, K. Jung, W.S. Son, *J. Kor. Magn. Reson. Soc*. **23**, 93 (2019)
23. Kim, J.H. Kim, *J. Kor. Magn. Reson. Soc*. **25**, 8 (2021)
24. M.I. Gordon, M.J.R. Hoch, *J. Phys. C: Solid State* Phys. **11**, 783 (1978)
25. A.R. Lim, S.H. Kim, S.Y. Jeong, *J. Mol. Struct.* **1031**, 234 (2013)
26. J.L. Koenig, *Spectroscopy of Polymers* (Elsevier, New York, 1999)
27. A.R. Lim, S.S. Park, J.H. Chang, *AIP Advances* **7**, 105018 (2017)